ACS chemical biology

Letters

pubs.acs.org/acschemicalbiology

Targeting the Early Step of Building Block Organization in Viral Capsid Assembly

Ayala Lampel,[†] Yaron Bram,[†] Anat Ezer,[†] Ronit Shaltiel-Kario,[†] Jamil S. Saad,[‡] Eran Bacharach,[§] and Ehud Gazit*[,†,∥]

[†]Department of Molecular Microbiology and Biotechnology, George S. Wise Faculty of Life Sciences, Tel Aviv University, Tel Aviv 69978, Israel

[‡]Department of Microbiology, University of Alabama at Birmingham, Birmingham, Alabama 35294, United States

[§]Department of Cell Research and Immunology, George S. Wise Faculty of Life Sciences, Tel Aviv University, Tel Aviv 69978, Israel

[∥]Department of Materials Science and Engineering, Iby and Aladar Fleischman Faculty of Engineering, Tel Aviv University, Tel Aviv 69978, Israel

Supporting Information

ABSTRACT: Viral assembly, similar to other self-organizing protein systems, relies upon early building blocks, which associate into the late supramolecular structures. An initial and crucial event during HIV-1 core assembly is the dimerization of the capsid protein C-terminal domain, which stabilizes the viral capsid lattice. Thus, monitoring and manipulating this stage is desirable both from mechanistic as well as clinical perspectives. Here, we developed a fluorescent-based method for the detection and visualization of these early capsid interactions. We detected strong dimeric interactions, which were influenced by mutations in the capsid protein. We utilized this assay for potential assembly inhibitors screening, which resulted in the identification of a leading compound that hinders the assembly of capsid protein *in vitro*. Moreover, a derivative of the compound impaired virus production and infectivity in cell cultures. These findings demonstrate that the described assay efficiently detects the very first association events in HIV-1 capsid formation and emphasize the significance of targeting early intermolecular interactions.

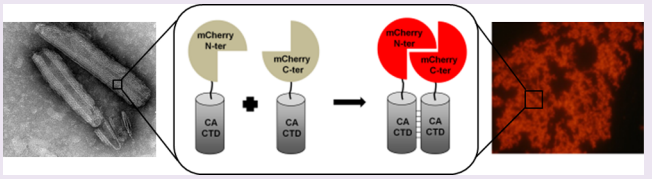

The organization of viral capsids by self-assembly of structural building blocks is a critical event in the viral replication cycle that carries major clinical implications. Similarly, the self-assembly of amyloid proteins is associated with many pathologies,[1] including Alzheimer's disease (AD), Parkinson's disease (PD), and type 2 diabetes (T2D). Targeting the initial steps of the association of these proteins holds an immense therapeutic potential yet is very challenging.

A major structural component of the human immunodeficiency virus-1 (HIV-1) is the capsid protein (CA) that assembles into the core encapsulating the viral genome and proteins.[2] CA comprises two independently folded domains, the N-terminal domain (NTD) and the C-terminal domain (CTD), separated by a flexible linker.[3−6] High-resolution structural models of HIV-1 core revealed that the lattice is formed by NTD hexamers, connected by CTD dimers.[7−9] The lattice-stabilizing CA CTD dimer interface is similar to the solution dimer interface,[8,10] indicating that the basic assembly unit of the HIV-1 core is composed of two CA subunits linked by their CTD. It was shown that mutations in CA CTD impair viral particle assembly both *in vitro* and *in vivo* and diminish viral infectivity,[4,11,12] thus, making the CTD dimerization an attractive therapeutic target.

A number of HIV-1 CA assembly inhibitors were previously reported,[13−19] demonstrating the antiviral potential of disrupting CA assemblies. To specifically target the CA dimerization event, we used bimolecular fluorescence complementation (BiFC) for the detection and visualization of this fundamental assembly unit. BiFC is based on the association of two nonfluorescent constituents fused to a protein of interest (here, the CA CTD) and the subsequent generation of a fluorescent complex as a result of interaction between the fused proteins.[20,21] This assay is widely used for protein−protein interactions and was recently utilized by us as a platform of high throughput screening (HTS) for amyloid assembly inhibitors.[22]

Following a screening for potential CA assembly inhibitors, we identified a leading compound which inhibits the assembly of CA protein *in vitro*. We found that a derivative of this compound inhibits assembly *in vitro* more efficiently as demonstrated by biophysical methods, including turbidity assay, dynamic light scattering (DLS), electron microscopy (EM), and nuclear magnetic resonance (NMR). We also found that this lead compound hinders viral infectivity and viral particle production in cell cultures, indicating the significance of targeting the initial CA interactions and the clinical relevance of the developed BiFC assay.

Received: April 7, 2015
Accepted: May 22, 2015
Published: May 22, 2015

DOI: 10.1021/acschembio.5b00347
ACS Chem. Biol. 2015, 10, 1785−1790

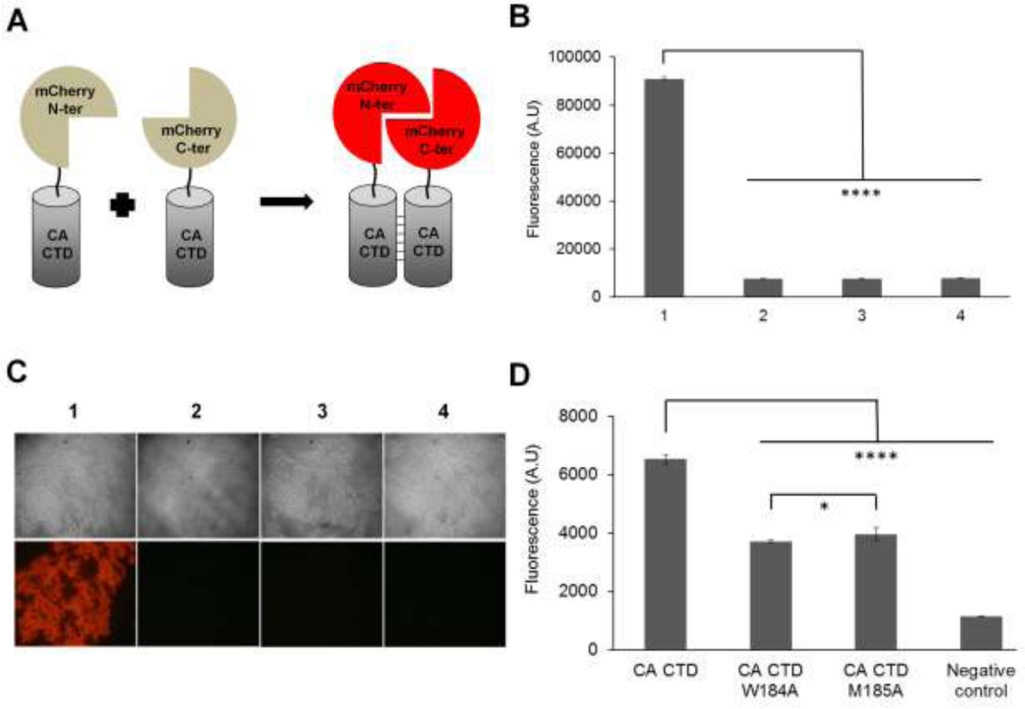

Figure 1. Detection of CA CTD intermolecular interactions using the BiFC assay. (A) Schematic representation of BiFC constructs. CA CTD (residues 146−231) fused to the N-terminus and C-terminus of mCherry fragments 1−159 (N-ter) and 160−237 (C-ter), respectively. Fluorescence spectroscopy (B) and fluorescence microscopy (C) of bacteria expressing the following pairs: CA CTD-N-ter and C-ter-CA CTD (1), mCherry N-ter and C-ter (2), CA CTD-N-ter and C-ter (3), or C-ter-CA CTD and N-ter (4). Upper panel: bright field. Lower panel: dark field. Magnification is ×40. (D) Fluorescence spectroscopy of bacteria expressing wild type or CA CTD mutants (either W184A or M185A) fused to split mCherry or the negative control (N-ter and C-ter). For B and D, excitation, 540/35; emission, 600/40. Values are means ± s.d., Student's *t* test, $^{*}P < 0.05$, $^{****}P < 0.0001$, $N = 4$.

To study and monitor the elementary association of CA CTD using BiFC, split mCherry protein, a mutant monomeric red fluorescent protein,[23] was used as the fluorescent marker. The two fragments of mCherry protein, residues 1−159 (N-ter) and 160−237 (C-ter), were cloned separately into *E. coli* expression vectors with compatible origins of replication (ORI).[22] CA CTD (residues 146−231, GeneBank accession number NP_579880) was fused to the mCherry fragments via a flexible linker consisting of two repeats of the sequence (Gly−Gly−Gly−Gly−Ser) (Figure 1A). To achieve efficient detection and visualization of CA CTD interactions and high expression of the assembly units, the assay was performed in bacteria cells (see Supporting Information). The fluorescence of *E. coli* cells expressing the CA CTD fused to the mCherry fragments was measured and compared to cells expressing the nonfused N-ter and C-ter mCherry fragments (negative control). To rule out the possibility that the fluorescent signal stems from interactions between CA CTD and mCherry fragments, two additional negative controls were examined—CA CTD fused to either the C-ter or the N-ter fragment coexpressed with the nonfused compatible mCherry fragment. As shown in Figure 1B, mCherry fragments carrying CA CTD generated a robust fluorescent signal, significantly higher than that of all negative controls, indicating no affinity between the individual mCherry fragments or between CA CTD and mCherry fragments. The fluorescence of CA CTD interactions could also be detected by fluorescence microscopy. Red fluorescence was evident in cells coexpressing the CA CTD-N-ter and C-ter-CA CTD fusions (Figure 1C, image 1), while no fluorescence was observed for cells expressing the negative controls (Figure 1C, images 2−4). These findings suggest that the fluorescent signal is the result of CA CTD interactions.

To evaluate the sensitivity of the BiFC assay in detecting alterations in CA CTD interactions, known mutations in the dimerization interface of CA CTD were also examined. As previously reported by structural and genetic data, Trp at position 184 (W184) and Met at position 185 (M185) have a significant role in CA CTD dimerization and in core organization.[4,11,24] Substitution of these residues to Ala significantly reduced CA CTD association (Figure 1D). The W184A mutation had a slightly stronger inhibitory effect than that of the M185A mutation. This finding is in agreement with previous studies showing that W184 is more critical for CA dimerization,[4] thus suggesting the BiFC system enables a sensitive detection of variations in CA association.

Next, we employed the assay to screen for potential inhibitors of CA CTD dimerization using a library of 1280 pharmacologically active compounds[22] (see Supporting Information, Table S1). This library offers high structural diversity; yet, for clinical purposes the positive hits should be medicinally modified to increase specificity for capsid protein, since these molecules have additional biological activity. The advantage of the designed BiFC assay as a screening method compared to other complementary methods such as co-immunoprecipitation[25] is that the assembled complex has strong intrinsic fluorescence, allowing direct visualization of CA CTD interaction with no need for exogenous agents.

Each compound was added in a final concentration of 100 μM to the media of cells expressing the CA CTD-mCherry constructs. To validate that the compounds directly affect CA

DOI: 10.1021/acschembio.5b00347
ACS Chem. Biol. 2015, 10, 1785−1790

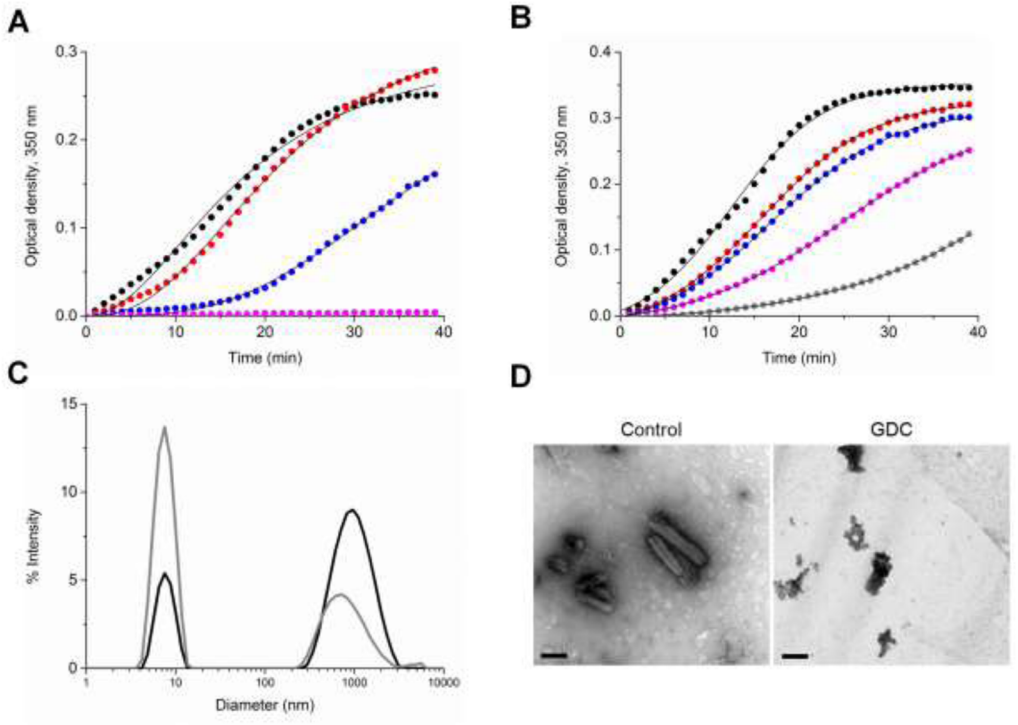

Figure 2. Effect of TA and TA derivatives on CA protein assembly *in vitro*. (A, B) Turbidity assay of CA protein assembly (38 μM, 2 M NaCl) in either the absence (black) or presence of (A) 2-fold (red), 10-fold (blue), or 100-fold (magenta) molar excess of TA; (B) 4-fold molar excess of GCA (red), TA (blue), TDC (magenta), or GDC (gray). (C) DLS analysis of CA assemblies (38 μM, 1.5 M NaCl) either in the absence (black) or presence (gray) of 4-fold molar excess of GDC. (D) TEM micrographs of CA assemblies (38 μM with 2 M NaCl) in the absence (control) or presence of 4-fold molar excess of GDC. Scale bar is 1 μm.

CTD interactions rather than other cellular processes such as protein translation or folding, the compounds were also added to cells expressing the intact mCherry protein. Each compound was tested in triplicate and normalized according to cell amount. The screening yielded four positive hits: taurocholic acid (TA), aminoguanidine hemisulfate (AGH), (±)-2-amino-5-phosphonopentanoic acid (A5PA), and acetylsalicylic acid (ASA). These compounds significantly inhibited CA CTD dimerization (by 50% or more; Figure S1) and had no significant effect on the intact mCherry protein (Figure S1).

Next, we examined whether the lead compounds inhibit the assembly of HIV-1 CA protein *in vitro*. The assembly of full-length HIV-1 CA protein was monitored over time either in the absence or in the presence of the compounds by turbidity assay. Quantitative analysis was obtained by fitting the time-dependent formation of light-scattering CA assemblies to a sigmoidal equation (Supporting Information). As shown in Figure S2 and Table S2, at a high molar excess of 100-fold, A5PA had no inhibitory effect on the assembly of the protein, as it increased the time at which the optical density reaches half of its final value (t_{50}) by 1.8-fold. However, AGH and ASA decreased the linear assembly rate by more than 2-fold and mildly increased the t_{50} of the reaction (Table S2). In contrast, TA significantly inhibited the assembly of CA protein, as all reactions, besides that with TA, reached equilibrium after 40 min. In addition, TA had no effect on the dimerization of two additional unrelated proteins, islet amyloid polypeptide, and α-synuclein,[22] further supporting specificity of the compound for capsid protein. The variance between the inhibitory performances of TA in the BiFC assay compared to that *in vitro* stresses the differences between the two systems; while the cellular bacterial milieu includes various factors that might affect the activity and affinity of TA to CA CTD such as molecular crowding or interactions with additional proteins, these factors do not occur in the *in vitro* settings.

TA was selected for further examination as the leading inhibitor. First, we studied the effect of varying TA concentrations on the assembly of CA; the compound inhibited CA protein association in a dose dependent manner (Figure 2A, Table S3). To further explore the activity of TA, we studied the inhibitory potential of three commercially available TA derivatives: glycocholic acid (GCA), taurodeoxycholate (TDC), and glycodeoxycholate (GDC; Figure S3). As shown in Figure 2B and Table S4, GDC had the most significant effect on CA protein assembly at 4-fold molar excess, as it decreased the assembly rate by 6-fold and increased the t_{50} by more than 4-fold. To determine the IC_{50} of GDC, the effect of varying concentrations of the compound on the linear assembly rate of CA protein was evaluated; the calculated IC_{50} of GDC *in vitro* was found to be 94.03 ± 0.56 μM (Figure S7A). The turbidity assay results suggest the compounds inhibit the lower scale aggregation of capsid protein. Size distribution of CA assemblies by DLS revealed that GDC increased the population of small particles and decreased the formation of large CA assemblies (Figure 2C). Ultrastructual analysis of CA assemblies demonstrated the formation of tubular structures resembling authentic cores after 30 min incubation of the protein in high ionic strength. Yet, in the presence of GDC, the protein failed to assemble into these organized structures (Figure 2D). The identical CD spectra of CA with or without GDC indicate that the CA structure is unchanged upon binding of GDC (Figure S4).

To gain more insights into the mechanism by which GDC disrupts CA assembly and to determine how GDC binds to the

DOI: 10.1021/acschembio.5b00347
ACS Chem. Biol. 2015, 10, 1785−1790

CA domain, we conducted NMR titration studies on the N-terminal and C-terminal domains of CA (NTD and CTD, respectively). As shown in Figure 3A, a subset of $^{1}H-^{15}N$

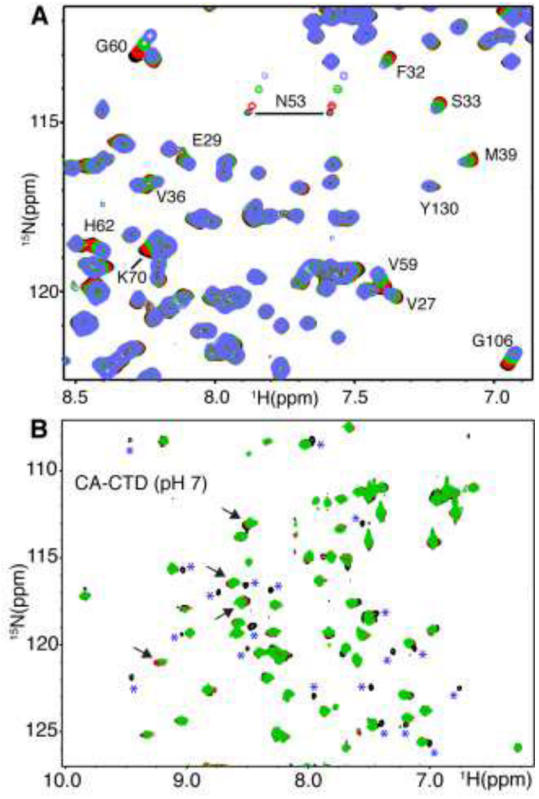

Figure 3. (A) Overlay of a selected region of 2D $^{1}H-^{15}N$ HSQC spectra for ^{15}N-labeled CA NTD (150 μM) at pH 5 upon increasing GDC concentration [GDC/NTD = 0:1 (black), 1:1 (red), 4:1 (green), and 8:1 (blue)]. (B) Overlay of a selected region of 2D $^{1}H-^{15}N$ HSQC spectra for ^{15}N-labeled CA CTD (150 μM) at pH 7 upon increasing GDC concentration [GDC/CTD = 0:1 (black), 4:1 (red), and 8:1 (green)]. Notice the disappearance of a subset of signals (denoted with asterisks) upon the addition of GDC. These signals are only observed when the solution pH of the CTD sample is ≥7. Other signals that exhibited chemical shift perturbations are indicated by arrows.

signals exhibited chemical shift changes upon increasing the concentration of GDC into a ^{15}N-labeled sample of NTD, indicating a direct and site-specific binding. Binding of GDC led to chemical shift perturbations for numerous residues such as T19, E29, K30, F32, S33, V36, F40, N53, L56, N57, V59, G60, G61, H62, Q63, A64, A65, K70, and G106. Interestingly, the majority of these residues are located in the binding site of the previously reported HIV-1 capsid assembly inhibitor, CAP1.[13] This was an unexpected result because GDC was expected to target the CTD domain. In the next experiment, we have titrated GDC into a ^{15}N-labeled sample of CA CTD at pH 7 followed by 2D HSQC experiments. Strikingly, a set of signals that is only observed at pH 7 disappeared upon the addition of an equimolar amount GDC (Figure 3B). The presence of an extra set of signals at pH 7 is consistent with previous studies indicating formation of CA CTD assemblies at pH 7.[26] Several other $^{1}H-^{15}N$ signals also exhibited chemical shift changes upon increasing the concentration of GDC (Figure 3B). GDC binding to CTD at pH 5 also led to perturbations of several $^{1}H-^{15}N$ resonances as observed for CTD at pH 7 (Figure S5). However, the extra set of signals is not observed at pH 5. These findings may suggest that GDC disrupts intermolecular interactions of CA CTD, as was demonstrated by the *in vitro* results and by the analysis in cell cultures. These findings indicate that GDC is able to bind to both NTD and CTD, suggesting a novel mechanism of inhibition. Additional structural studies will be conducted in the future to obtain more details into the mechanism of GDC binding.

To study the effect of GDC on viral infectivity, 293T cells were cotransfected with plasmids encoding for vesicular stomatitis virus envelope glycoprotein (VSV-G), HIV-1 Gag and Pol proteins (pCMVΔR8.2), and a retroviral vector encoding for green fluorescent protein (GFP, pHR'CMV-GFP; Supporting Information). Five hours post-transfection, cells were treated with varying concentrations of GDC. Supernatants containing virus-like particles (VLPs) were collected 48 h post-transfection; these samples were used to infect naïve 293T cells. Infection levels were determined 48 h postinfection by measuring the reporter GFP-positive cells using fluorescence-activated cell sorting (FACS). As shown in Figure 4A, GDC decreased the infectivity in a dose dependent manner by ∼20%, 62%, and 89% at 1 μM, 5 μM, and 50 μM, respectively, while a complete inhibition of infectivity was observed at 200 μM. The IC_{50} of GDC from the infectivity assay, which was found to be 3.12 ± 0.37 μM, was calculated by fitting the inhibition of infectivity values (100-relative infectivity) for each of the GDC concentrations to a sigmoidal equation (Figure S7B). The antiviral activity of GDC was compared to that of CAP-1,[13] which failed to inhibit viral infectivity at 50 μM (Figure 4A). The IC_{50} of GDC from the infectivity assay is in the same scale of the previously reported CA assembly inhibitors IC_{50} values, including benzodiazepines, benzimidazoles and their analogues (IC_{50} = 0.35−6.1 μM),[18] acylhydrazone compounds (IC_{50} = 0.41−14.86 μM),[19] and the modified 12-mer helical peptide CAI,[16] NYAD-1 (IC_{50} = 4−15 μM).[27] However, the IC_{50} of GDC is higher than that reported by Blair and colleagues of the assembly inhibitor PF-3450074 (IC_{50}0.08−0.64 μM).[14] The direct effect of GDC on cell viability was tested by 2,3-bis(2-methoxy-4-nitro-5-sulfophenyl)-2H-tetrazolium-5-carboxanilide (XTT) assay. At concentrations of up to 25 μM, GDC had no significant toxic effect; however, cell viability was decreased by 9%, 10%, and 19% at 50 μM, 100 μM, and 200 μM, respectively. CAP-1, in contrast, decreased cell viability by 15% at 25 μM and by more than 50% at 200 μM (Figure S6). Next, to inspect whether GDC antiviral activity is mediated by interference with viral assembly, we purified virions produced by 293T cells incubated either in the absence or presence of varying concentrations of GDC. Capsid protein levels inside the cells media were analyzed by Western blot assay using an antibody against HIV-1 CA protein. This analysis confirmed that GDC decreased capsid levels, suggesting that the compound reduces extracellular virion levels (Figure 4B). GDC treatment did not affect intracellular actin levels, as judged by immunoblotting, using antiactin antibody, in contrast to CAP-1 treatment that mildly reduced the levels of this cellular protein (data not shown). This indicates that GDC treatment was not toxic to the cells. Intracellular Gag levels, normalized to actin levels, were not changed by GDC (or CAP-1) treatment, and accordingly, the dose-dependent effect of GDC on extracellular capsid levels was calculated relative to the normalized intracellular Gag levels (Figure 4C). Altogether, the remarkable correlation between reduced infectivity and reduced extracellular capsid levels suggests that GDC inhibits HIV

DOI: 10.1021/acschembio.5b00347
ACS Chem. Biol. 2015, 10, 1785−1790

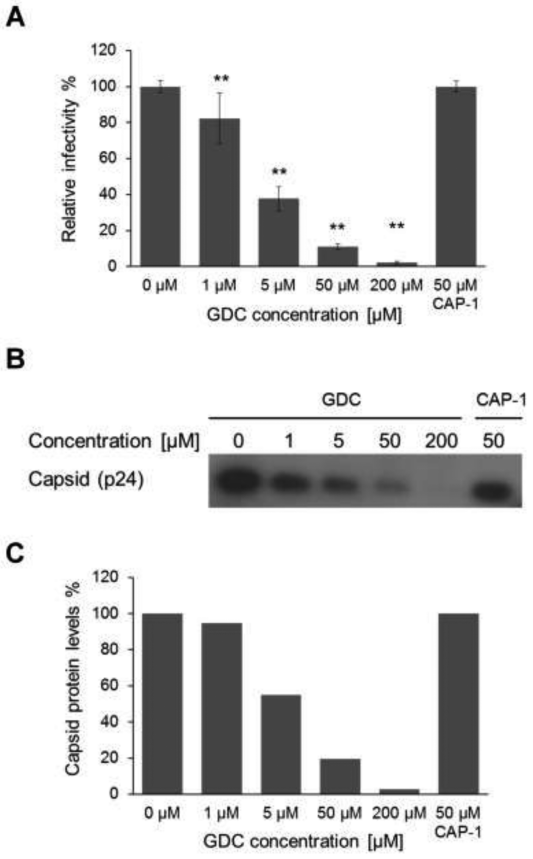

Figure 4. Effect of GDC on viral infectivity and assembly. (A) 293T cells transfected with plasmids expressing components of the HIV-1-based vector system were incubated either in the absence or presence of varying concentrations of GDC or with CAP-1 (50 μM). Virions in culture supernatants, normalized according to GFP levels, were used to infect naïve 293T cells, which were analyzed by FACS 48 h postinfection. The relative infectivity is the percentage of infectivity for compound-treated samples compared to untreated samples. Bars and error bars represent mean and SD, respectively; $n = 3$, Student's t test, $^{**}P < 0.01$. (B) Western blot analysis of capsid protein levels from purified virions produced by 293T cells that were treated with the indicated compound concentrations, analyzed by an anticapsid antibody. (C) Calculation of extracellular capsid levels in respect to intracellular Gag levels. Densitometry of immunoblots, using anticapsid antibody, was used to quantify both capsid levels in virion pellets (B) and Gag levels in extracts of transfected 293T cells, treated with the indicated GDC or CAP-1 concentrations. Actin levels were detected using antiactin antibody and were used as an internal control for the cellular protein levels. For each sample, percentages of capsid levels were calculated by the following equation: 100 × (extracellular capsid levels)/(intracellular Gag levels, normalized by actin levels).

infectivity by interfering with the Gag assembly, likely by hindering capsid-mediated Gag−Gag interactions. This scenario is in line with the direct binding of GDC to both NTD and CTD of the capsid, since both domains participate in Gag−Gag interactions.[28] The inhibitory effect of GDC on the *in vitro* assembly of capsid (see above) further suggests that GDC may have an additional negative effect on virion maturation of particles that did assemble. The lower efficiency of GDC inhibitory activity *in vitro* (IC_{50} = ~94 μM) as compared to *in cellulo* (IC_{50} = ~3 μM) suggests that the compound inhibits viral production by an additional route, presumably by interfering with other viral factors such as the viral enzymes. Further examination is needed to inspect this proposed additional activity of GDC.

In summary, the main advantage of the newly developed BiFC assay relies upon the ability to detect the very first intermolecular interactions in the assembly process of the HIV-1 CA protein, events that are usually difficult to observe by other methods. This is the first assay reported to date of screening for assembly inhibitors that specifically target the essential CA CTD dimerization. This work led to the identification of a potential antiviral compound that inhibits viral particle organization, further demonstrating the significant role of CA CTD dimerization in HIV-1 assembly. Since viral assembly is pivotal for the formation of functional particles, this system should provide a platform for screening antiviral drugs against the building blocks of other pathogenic viruses as well.

METHODS

All experimental procedures are found in the Supporting Information.

ASSOCIATED CONTENT

Supporting Information

Supporting Information includes experimental methods, supplementary figures and tables. The Supporting Information is available free of charge on the ACS Publications website at DOI: 10.1021/acschembio.5b00347.

AUTHOR INFORMATION

Corresponding Author

*E-mail: ehudg@post.tau.ac.il.

Author Contributions

The manuscript was written through contributions of all authors. All authors have given approval to the final version of the manuscript.

Notes

The authors declare no competing financial interest.

ACKNOWLEDGMENTS

This work was supported in part by grants from the Israeli National Nanotechnology Initiative and Helmsley Charitable Trust for a focal technology area on Nanomedicines for Personalized Theranostics and the Israel Academy of Sciences and Humanities, Batsheva de Rothschild Fund, Aharon and Ephraim Katzir Fellowship. We are grateful to W. I. Sundquist and P. E. Prevelige, Jr. for the CA plasmid constructus, to O. Sagi-Assif for the assistance with the FACS analysis, to S. Perov and I. Levinzon for the assistance with the *in vitro* analysis of CA protein assembly, and to members of the Gazit laboratory for helpful discussions.

ABBREVIATIONS

CA, capsid protein; CTD, C-terminal domain; NTD, N-terminal domain; BiFC, bimolecular fluorescence complementation; DLS, dynamic light scattering; TEM, transmission electron microscopy; NMR, nuclear magnetic resonance

REFERENCES

(1) Eisenberg, D., and Jucker, M. (2012) The amyloid state of proteins in human diseases. *Cell 148*, 1188−1203.

(2) Göttlinger, H. G. (2001) The HIV-1 assembly machine. *Aids 15*, S13−S20.

DOI: 10.1021/acschembio.5b00347
ACS Chem. Biol. 2015, 10, 1785−1790

(3) Gamble, T. R., Vajdos, F. F., Yoo, S., Worthylake, D. K., Houseweart, M., Sundquist, W. I., and Hill, C. P. (1996) Crystal structure of human cyclophilin A bound to the amino-terminal domain of HIV-1 capsid. *Cell 87*, 1285−1294.
(4) Gamble, T. R., Yoo, S., Vajdos, F. F., von Schwedler, U. K., Worthylake, D. K., Wang, H., McCutcheon, J. P., Sundquist, W. I., and Hill, C. P. (1997) Structure of the carboxyl-terminal dimerization domain of the HIV-1 capsid protein. *Science 278*, 849−853.
(5) Momany, C., Kovari, L. C., Prongay, A. J., Keller, W., Gitti, R. K., Lee, B. M., Gorbalenya, A. E., Tong, L., McClure, J., Ehrlich, L. S., Summers, M. F., Carter, C., and Rossmann, M. G. (1996) Crystal structure of dimeric HIV-1 capsid protein. *Nat. Struct. Biol. 3*, 763−770.
(6) Gitti, R. K., Lee, B. M., Walker, J., Summers, M. F., Yoo, S., and Sundquist, W. I. (1996) Structure of the amino-terminal core domain of the HIV-1 capsid protein. *Science 273*, 231−235.
(7) Pornillos, O., Ganser-Pornillos, B. K., Kelly, B. N., Hua, Y., Whitby, F. G., Stout, C. D., Sundquist, W. I., Hill, C. P., and Yeager, M. (2009) X-ray structures of the hexameric building block of the HIV capsid. *Cell 137*, 1282−1292.
(8) Ganser-Pornillos, B. K., Cheng, A., and Yeager, M. (2007) Structure of full-length HIV-1 CA: a model for the mature capsid lattice. *Cell 131*, 70−79.
(9) Zhao, G. P., Perilla, J. R., Yufenyuy, E. L., Meng, X., Chen, B., Ning, J. Y., Ahn, J., Gronenborn, A. M., Schulten, K., Aiken, C., and Zhang, P. (2013) Mature HIV-1 capsid structure by cryo-electron microscopy and all-atom molecular dynamics. *Nature 497*, 643−646.
(10) Byeon, I.-J. L., Meng, X., Jung, J., Zhao, G., Yang, R., Ahn, J., Shi, J., Concel, J., Aiken, C., Zhang, P., and Gronenborn, A. M. (2009) Structural convergence between Cryo-EM and NMR reveals intersubunit interactions critical for HIV-1 capsid function. *Cell 139*, 780−790.
(11) von Schwedler, U. K., Stray, K. M., Garrus, J. E., and Sundquist, W. I. (2003) Functional surfaces of the human immunodeficiency virus type 1 capsid protein. *J. Virol. 77*, 5439−5450.
(12) Burniston, M. T., Cimarelli, A., Colgan, J., Curtis, S. P., and Luban, J. (1999) Human immunodeficiency virus type 1 Gag polyprotein multimerization requires the nucleocapsid domain and RNA and is promoted by the capsid-dimer interface and the basic region of matrix protein. *J. Virol. 73*, 8527−8540.
(13) Tang, C., Loeliger, E., Kinde, I., Kyere, S., Mayo, K., Barklis, E., Sun, Y., Huang, M., and Summers, M. F. (2003) Antiviral inhibition of the HIV-1 capsid protein. *J. Mol. Biol. 327*, 1013−1020.
(14) Blair, W. S., Pickford, C., Irving, S. L., Brown, D. G., Anderson, M., Bazin, R., Cao, J., Ciaramella, G., Isaacson, J., Jackson, L., Hunt, R., Kjerrstrom, A., Nieman, J. A., Patick, A. K., Perros, M., Scott, A. D., Whitby, K., Wu, H., and Butler, S. L. (2010) HIV capsid is a tractable target for small molecule therapeutic intervention. *PLoS Pathog. 6*, e1001220.
(15) Cao, J., Isaacson, J., Patick, A. K., and Blair, W. S. (2005) High-throughput human immunodeficiency virus type 1 (HIV-1) full replication assay that includes HIV-1 Vif as an antiviral target. *Antimicrob. Agents Chemother. 49*, 3833−3841.
(16) Sticht, J., Humbert, M., Findlow, S., Bodem, J., Muller, B., Dietrich, U., Werner, J., and Krausslich, H.-G. (2005) A peptide inhibitor of HIV-1 assembly in vitro. *Nat. Struct. Mol. Biol. 12*, 671−677.
(17) Curreli, F., Zhang, H., Zhang, X., Pyatkin, I., Victor, Z., Altieri, A., and Debnath, A. K. (2011) Virtual screening based identification of novel small-molecule inhibitors targeted to the HIV-1 capsid. *Bioorg. Med. Chem. 19*, 77−90.
(18) Fader, L. D., Bethell, R., Bonneau, P., Bös, M., Bousquet, Y., Cordingley, M. G., Coulombe, R., Deroy, P., Faucher, A.-M., Gagnon, A., Goudreau, N., Grand-Maître, C., Guse, I., Hucke, O., Kawai, S. H., Lacoste, J.-E., Landry, S., Lemke, C. T., Malenfant, E., Mason, S., Morin, S., O'Meara, J., Simoneau, B., Titolo, S., and Yoakim, C. (2011) Discovery of a 1, 5-dihydrobenzo [b][1, 4] diazepine-2, 4-dione series of inhibitors of HIV-1 capsid assembly. *Bioorg. Med. Chem. Lett. 21*, 398−404.
(19) Jin, Y., Tan, Z., He, M., Tian, B., Tang, S., Hewlett, I., and Yang, M. (2010) SAR and molecular mechanism study of novel acylhydrazone compounds targeting HIV-1 CA. *Bioorg. Med. Chem. 18*, 2135−2140.
(20) Shekhawat, S. S., and Ghosh, I. (2011) Split-protein systems: beyond binary protein-protein interactions. *Curr. Opin. Chem. Biol. 15*, 789−797.
(21) Kerppola, T. K. (2006) Visualization of molecular interactions by fluorescence complementation. *Nat. Rev. Mol. Cell. Biol. 7*, 449−456.
(22) Bram, Y., Lampel, A., Shaltiel-Karyo, R., Ezer, A., Scherzer-Attali, R., Segal, D., and Gazit, E. (2015) Monitoring and Targeting the Initial Dimerization Stage of Amyloid Self-Assembly. *Angew. Chem., Int. Ed. 54*, 2062−2067.
(23) Fan, J.-Y., Cui, Z.-Q., Wei, H.-P., Zhang, Z.-P., Zhou, Y.-F., Wang, Y.-P., and Zhang, X.-E. (2008) Split mCherry as a new red bimolecular fluorescence complementation system for visualizing protein−protein interactions in living cells. *Biochem. Biophys. Res. Commun. 367*, 47−53.
(24) Melamed, D., Mark-Danieli, M., Kenan-Eichler, M., Kraus, O., Castiel, A., Laham, N., Pupko, T., Glaser, F., Ben-Tal, N., and Bacharach, E. (2004) The conserved carboxy terminus of the capsid domain of human immunodeficiency virus type 1 gag protein is important for virion assembly and release. *J. Virol. 78*, 9675−9688.
(25) Aggarwal, V., and Ha, T. (2014) Single-molecule pull-down (SiMPull) for new-age biochemistry. *BioEssays 36*, 1109−1119.
(26) Ehrlich, L. S., Liu, T., Scarlata, S., Chu, B., and Carter, C. A. (2001) HIV-1 capsid protein forms spherical (immature-like) and tubular (mature-like) particles in vitro: structure switching by pH-induced conformational changes. *Biophys. J. 81*, 586−594.
(27) Zhang, H., Zhao, Q., Bhattacharya, S., Waheed, A. A., Tong, X., Hong, A., Heck, S., Curreli, F., Goger, M., and Cowburn, D. (2008) A cell-penetrating helical peptide as a potential HIV-1 inhibitor. *J. Mol. Biol. 378*, 565−580.
(28) Schur, F. K. M., Hagen, W. J. H., Rumlová, M., Ruml, T., Müller, B., Kräusslich, H.-G., and Briggs, J. A. G. (2015) Structure of the immature HIV-1 capsid in intact virus particles at 8.8 A resolution. *Nature 517*, 505−508.

DOI: 10.1021/acschembio.5b00347
ACS Chem. Biol. 2015, 10, 1785−1790